The Origin of the Remarkable Regioselectivity of Fe^+-Mediated Dehydrogenation in Benzocycloalkenes

Roland H. Hertwig, Katrin Seemeyer, Helmut Schwarz,* and Wolfram Koch*

Abstract: Combined mass spectrometric experiments and density functional theory (DFT) calculations have been performed to determine the regioselectivity and uncover the origin of the C–H bond activation of benzocycloalkenes by "bare" Fe^+ cations. The hydrocarbons investigated are benzocyclohexene, -heptene, and -octene. Extensive labeling experiments demonstrate that the site of C–H bond activation in the non-aromatic ring is dependent on the ring size. The barriers for the dehydrogenation process as predicted by DFT calculations are in agreement with the experimental findings. Further, the combined experimental and theoretical approach applied in the present study allows the principles underlying the remarkable ring size dependent regioselectivity of C–H bond activation in these hydrocarbons to be unraveled.

Keywords
C–H activation · density functional calculations · gas-phase chemistry · mass spectrometry · transition metals

Introduction

Activation of inert C–H bonds by "bare" transition-metal cations has emerged as a rich branch of organometallic chemistry since its discovery by Allison, Freas, and Ridge in 1979.[1] In fact, gas-phase experiments in general and mass spectrometry based studies in particular have produced a wealth of information on reactions of "bare" and/or ligated transition-metal ions with organic substrates.[2] While these investigations yield thermochemical and structural information about the entrance and exit channels, quite often, they fail to provide any insight into mechanistic and thermodynamic aspects of the reactive intermediates and transition states of such reactions. Understanding the latter is a prerequisite for the de novo design of the reaction centers of catalysts, which almost always contain transition metals. Theoretical studies can contribute towards this, provided that the methods employed are judiciously chosen to suit the problem. Unfortunately, this goal is not easy to achieve for coordinatively unsatured transition-metal hydrocarbon complexes, because dynamic and static electron correlation effects both play an important role,[3] and within the framework of post-Hartree–Fock methods a high level of sophistication is required to treat correlation effects accurately. This is one of the reasons why, in the past, the application of theory was confined to rather small systems. Density functional theory (DFT)[4] affords an implicit treatment of electron correlation at a computational cost comparable to that of simple Hartree–Fock calculations. Recently, numerous studies have shown that modern density functionals, either pure DFT or ACM (adiabatic connection or HF/DFT hybrid) methods, are useful approximations for the treatment of transition-metal complexes,[5] even for the demanding open-shell situation discussed here.[6–9]

In this study, we present a combined mass spectrometric and quantum chemical investigation on the Fe^+-mediated dehydrogenation of tetralin and its homologues benzocycloheptene and -octene. The gas-phase labeling experiments show distinct differences depending on the position of the double bond generated in the course of the reaction, and a remarkable ring-size effect prevails. The origin of this effect has been uncovered by DFT calculations, which, together with thermochemical data, provide structural information for the most important stationary points of the dehydrogenation reactions.

Methods

As the experimental setup has been described previously in detail,[10] only a brief description will be given. A 1:1 mixture of $Fe(CO)_5$ and the benzocycloalkene or its deuterated derivative was bombarded with 100 eV electrons in the chemical ionization source (repeller voltage ca. 0 V) of a modified four-sector tandem mass spectrometer of BEBE configuration (B stands for magnetic and E for electric sector), in which MS-I is the original VG ZAB-HF-2F part and MS-II is an AMD 604 mass spectrometer. Although the actual mechanism by which the complexes are formed is yet unknown, the pressure in the ion source is high enough to permit collisional cooling thus increasing the lifetime such that time-delayed decomposition reactions take place after ca. 1 μs (metastable ion (MI) dissociation). To this end, the organometallic complexes of Fe^+ and the benzocycloalkene having 8 keV translational energy were mass-selected by means of B(1)E(1). Unimolecular reactions occurring in the field-free region between E(1) and B(2) were record-

[*] H. Schwarz, W. Koch, R. H. Hertwig, K. Seemeyer
Institut für Organische Chemie der Technischen Universität Berlin
Straße des 17. Juni 135, 10623 Berlin (Germany)
Fax: Int. code +(30)3142-1102
e-mail: kochw@argon.chem.tu-berlin.de

ed by scanning B(2). Spectra were recorded on-line and averaged by using signal-averaging techniques employing the AMD Intectra data system. In typical experiments, 15–20 spectra were accumulated, and the error is not expected to exceed ±10%. All compounds were synthesized by standard laboratory procedures, purified by chromatographic means and fully characterized by spectroscopic methods. A full account of the synthesis is given in ref. [10c].

In the computational calculations, we applied the local spin density functional approximation (LSDA)[11] augmented by nonlocal corrections for exchange and correlation according to Becke[12] and Perdew[13] (BP). The nonlocal corrections were included self-consistently in the SCF calculations. A finer grid than default was used in the integration of the charge density to reduce the numerical error in the gradient calculations. Preoptimization and generation of a Hessian matrix using MNDO/d[14] was of great help in speeding up the DFT optimizations. The calculations were carried out utilizing the UniChem/DGauss package[15] employing the DZVP2 all-electron basis set[16] option implemented in the program. This basis set represents a (15s,9p,5d)/[5s,3p,2d] expansion of gaussian basis functions for the iron, and (10s,6p,1d)/[3s,2p,1d] and (5s,1p)/[2s,1p] expansions for carbon and hydrogen, respectively, and was specifically designed for use with DFT methods. In addition, it is augmented by a set of auxiliary basis functions to be used in a Coulomb potential fit procedure. The calculations involved up to 289 contracted gaussian functions (329 primitive functions) and 527 fit basis functions for the largest complexes. All geometries were fully optimized employing analytical gradient techniques without imposing symmetry constraints. Second derivatives of the energy with respect to the DFT optimized Cartesian coordinates were calculated analytically to identify genuine minima or saddle points and to obtain zero-point vibrational energy (ZPVE) corrections. In a previous study,[9] we reported on the ground state structures and energies of complexes of cationic iron with tetralin (**1**) and its dehydrogenated derivatives dihydronaphthalene (**2**) and naphthalene (**4**) using similar techniques. However, since analytic second derivatives were not available at that time and a numerical calculation of the Hessian matrix clearly exceeded the allocated computer resources, no ZPVE corrections were included in this earlier work. Also, the calculation and identification of saddle points was not feasible in the absence of second derivatives. The calculations were performed on a CRAY J916/32-8192 at the Konrad Zuse Zentrum für Informationstechnik (ZIB) in Berlin and on various CRAY C90 and T90 machines at the CRAY Research computing facilities in Eagan, MN, USA.

Table 1. Unimolecular, Fe^+-induced dehydrogenation of benzocyclohexene (**1**), -heptene (**5**), and -octene (**10**) and their isotopologues [a].

		Δm				
		2	3	4	5	6
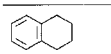	**1**	35		65		
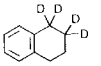	**1a**	37		8		55
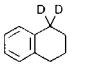	**1b**	29	12		59	
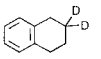	**1c**	29	12		59	
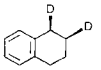	**1d[b]**	41		43		16
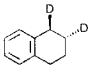	**1e[b]**	31	12		57	
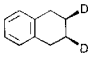	**1f**	29	8	44		19
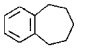	**5**	100				
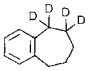	**5a**	67	29	4		
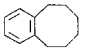	**10**	100				
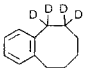	**10a**	100				
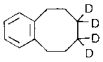	**10b**			100		
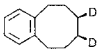	**10c[c]**	42		58		

[a] Data are normalized to $\sum$ fragment = 100%; the data for **1**–**1f** are taken from ref. [10c,9,17]. [b] Compounds **1d** and **1e** were studied as racemic pairs. [c] The ratio of H_2 versus D_2 losses from the Fe^+ complexes of **10c** dependends on the lifetime of the metastable ions: for dissociations in the first field-free region it is 52:48, in the second 50:50, and in the third 42:58; for a discussion of the origin of this effect, see ref. [10c].

Experimental Results

Since the experimental results of the Fe^+-mediated dehydrogenation of tetralin (**1**) have been reported previously,[9, 17] only a brief summary is given here. Extensive regio- and stereospecific labeling experiments (Table 1) demonstrate the following: The reaction is both regio- and stereospecific, leading first to the Fe^+ complex of 1,2-dihydronaphthalene (**2**) and finally to Fe^+–naphthalene (**4**–Fe^+). Dehydrogenation of the C2/C3 protons giving rise to **3**–Fe^+ does not take place (Figure 1). Also, 1,4-elimination of molecular hydrogen, involving for example C1/C4, can be ruled out, and the Fe^+-mediated reaction follows a clean 1,2-*syn*-elimination of molecular hydrogen. Finally, detailed experiments demonstrate that during the course of the reaction the metal ion sticks to the same face of the hydrocarbon surface.

For the next higher homologue, that is, benzocycloheptene (**5**), 1,2-*syn*-elimination involves both C1/C2 and C2/C3; if one ignores the operation of a kinetic isotope effect, the latter path is slightly favored (58% versus 42%, see also footnote [c] in Table 1). In contrast to the Fe^+–tetralin system, no further dehydrogenation to form the Fe^+ complexes of **8** or **9** is observed (Figure 1).

The behavior of benzocyclooctene (**10**) is again different in that the activated benzylic C–H bond (C1) and the homobenzylic C–H bond (C2) are not at all involved in the Fe^+-mediated dehydrogenation. Instead, molecular hydrogen originates exclusively from the C3/C4 positions and stereospecific labeling suggests the operation of a clean 1,2-*syn*-elimination in the generation of **13**–Fe^+. As with **5**, in the higher homologue **10**, there are no indications for consecutive dehydrogenation to form any of the Fe^+ complexes of **14**, **15**, or **16**.

In contrast to the behavior of **1**–Fe^+, the results obtained for the C–H bond activation of the benzocycloheptene (**5**) and –octene (**10**) systems contradict chemical intuition and textbook knowledge, which would predict a high preference for reaction of the metal cation at the benzylic position for the following reasons: 1) as the iron is bound to the aromatic part of the molecule, reaction is likely to occur at positions adjacent to this moiety; 2) the reaction of Lewis acids at the benzylic position is favored by electronic factors. In our previous study of the **1**–Fe^+ system,[9] we found that the iron is most likely to be ligated to the benzene ring, and the same principles are expected to apply in **5**–Fe^+ and **10**–Fe^+. Also, the extension of the nonaromatic ring by one or two CH_2 units is not expected to have

© VCH Verlagsgesellschaft mbH, D-69451 Weinheim, 1997 0947-6539/97/0308-1316 $ 17.50+.50/0 Chem. Eur. J. 1997, 3, No. 8

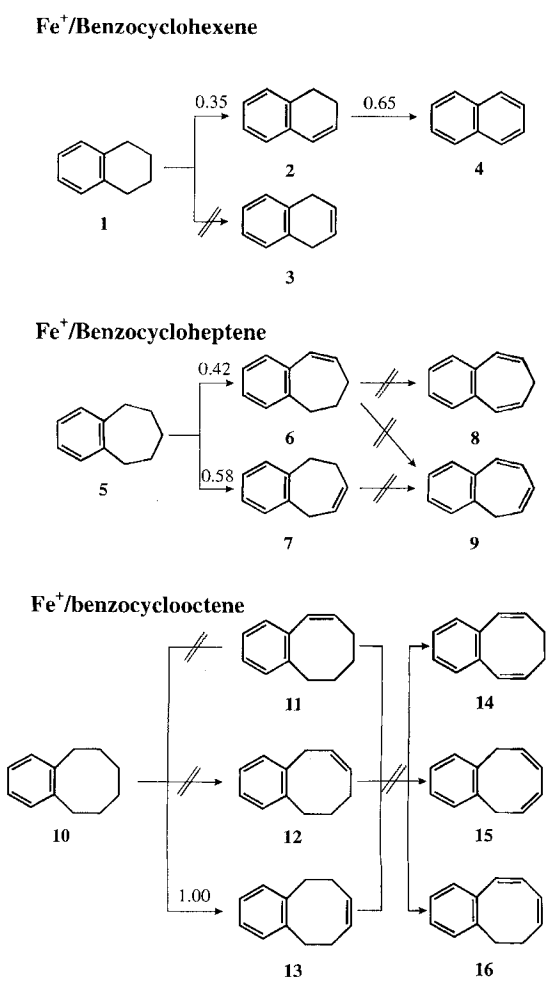

Figure 1. Possible and observed dehydrogenation products and product ratios as determined by mass spectrometric labeling experiments [10c·9·17].

a significant influence on the preferred reaction site, since the geometry of the aliphatic part of the molecule was found to be more or less unaffected by the presence of the iron cation in **1**–Fe^+.[9] It is therefore not clear whether conformational aspects alone can explain the remarkable effect that ring size has on the regioselectivity of C–H bond activation in **5** and **10**, and it seems likely that other kinetic factors play a role, especially in the case of the second dehydrogenation, which is only observed for tetralin (**1**). The aim of the theoretical calculations described below is to shed some light on the different reactivities observed experimentally and to clarify the origin of this behavior.

Computational results

Since the molecules discussed here are rather demanding, both theoretically and computationally, we would like to start this section by briefly describing the obstacles we faced and the strategies we used to circumvent them. First of all, we had to ensure that the theoretical approach chosen would be adequate in tackling our system. Owing to the open-shell character and the unsaturated ligand sphere of the complexes examined, a large number of energetically near-degenerate electronic states exist; substantial dynamic as well as nondynamic correlation effects are therefore expected to operate. An adequate theoretical description of such complicated electronic systems must include these effects and, as mentioned in the introduction, only high-level multi-reference CI methods afford this in a straightforward manner. Since calculations of this sort are technically beyond reach for large molecules, we had to find a level of theory that balanced computational demand with the quality of the results, so as to obtain a useful level of accuracy at a reasonable price. Modern density functional theory (DFT) methods take into account exchange and correlation effects in an implicit, approximate manner and furnish results that are in many cases in good agreement with experimental and high-level ab initio results, as shown in recent reviews on the applicability of DFT to transition-metal systems.[7, 18] Also, while substantial spin contamination may often be detrimental to the results within the UHF formalism, this is actually much less of a problem in unrestricted Kohn–Sham calculations.[19] In fact, in none of our calculations did the $\langle S^2 \rangle$ expectation values deviate from the exact eigenvalue by more than 0.05.

But even with relatively fast DFT methods, a complete investigation of all relevant points on the PES of each of the three Fe^+ complexes of **1**, **5**, and **10** would demand an enormous amount of computational resources, because of the large number of stationary points that lie on or in the vicinity of the assumed reaction pathway, not to speak of the size and low symmetry of these systems. Therefore, handling this problem from a theoretical point of view would be impossible without prior knowledge of the elementary mechanistic steps involved in C–H bond activations mediated by metal ions. Fortunately, the relevant details have recently been published for the model systems Fe^+/ethane and Fe^+/propane.[8] In these theoretical studies, it was demonstrated that, after insertion of Fe^+ into a C–H bond, the reaction proceeds via a concerted multicenter transition state, leading to the extrusion of molecular hydrogen (Figure 2).

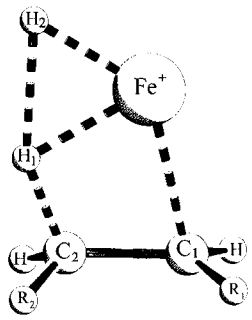

Figure 2. Multicenter transition-state structure for the rate-determining step of Fe^+-mediated C–H bond activation in alkanes.

The often-invoked[2] high-valent intermediates $R-Fe(H)_2^+$ (R = organic residue) were not found to correspond to minima. This key feature of C–H bond activation (Figure 2) should in principle be transferable to larger and more complicated organic substrates, provided that the following is taken into account:

1) Ligands bearing functional groups (e.g. double bonds) may slightly alter the transition-state structure by additional interaction with the metal center.
2) With increasing size of the organic ligand the number of possible sites for C–H bond insertion will grow, and the potential energy surface will be much more complex as a result.
3) The energetics of all possible reaction channels are of interest, when considering the product ratios found in the gas-phase experiments. This information and the electronic structures of intermediates and transition-state structures provide the link between the encounter and the product complexes.

In the current investigation only the potential energy surfaces of quartet multiplicity have been considered. In our previous study,[9] we also computed species with five unpaired electrons (sextet state), but found them to be higher in energy. This is in line with the results of Holthausen et al.[8] for Fe^+/C_2H_6 and Fe^+/C_3H_8 and Bauschlicher et al. for the Fe^+/benzene complex,[20] where the quartet states were always lowest in energy. Figure 3 shows schematically the possible pathways for C–H bond activation in benzocycloalkenes by a coordinatively unsaturated Fe^+ cation attached to the π system. In the course of the dehydrogenation process, the Fe^+ cation may bend towards a specific reaction site in the aliphatic part of the molecule or else the organic ligand may change its conformation in such a way that a given C–H bond approaches the iron atom.

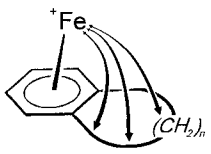

Figure 3. Possible insertion sites for Fe^+-mediated dehydrogenation of benzocycloalkenes **1** (n = 4), **5**, (n = 5), and **10** (n = 6).

What are the factors that determine the relative energies of the saddle points for the possible sites of attack shown in Figure 3? To answer this question, we must consider that in all the Fe^+–benzocycloalkene complexes the iron is initially bound to the aromatic ring in a η^6 fashion[9, 20] and is thus far removed from the reaction site located in the non-aromatic part of the organic ligand. If the iron cation migrates to the insertion site, it will, at least partially, loose its stabilizing interaction with the benzenoid π system. If, on the other hand, the organic ligand undergoes conformational changes so that insertion into a given C–H bond and subsequent formation of the crucial transition state (Figure 3) become geometrically feasible, the ligand structure must be perturbed from its minimum-energy geometry. Both these scenarios involve an increase in energy; which pathway or even combination of pathways prevails depends the relative energies required for these perturbations from the equilibrium geometry. Since benzocycloalkenes offer several sites for C–H bond activation, different products may form through the various possible dehydrogenation pathways, which are likely to differ in the energy required to overcome the barrier to bond activation. Moreover, it is to be expected that different ligands (i.e. **1**, **5**, and **10**) will differ in their preference for a specific reaction site.

The energetically most ideal situation will arise when the non-aromatic ring is flexible enough to bring one of its CH_2 units into the vicinity of the η^6-coordinated iron, since this allows the iron to maintain its energetically favorable position. The worst case will arise when the aliphatic section of the ligand is rigid or when a given CH_2 unit cannot bend towards the iron cation without generating too much strain in the non-aromatic ring; the iron would then have to give up its stabilizing coordination with the aromatic π system to migrate to the insertion site. In between these two extremes, several scenarios are conceivable, involving a mutual motion of iron cation and CH_2 unit towards each other. One way of determining the reaction pathways with the lowest barriers for benzocyclohexene (**1**), benzocycloheptene (**5**), and benzocyclooctene (**10**) would of course be to calculate all stationary points for all possible reactions shown in Figure 1. This "sledgehammer" approach can be avoided by using the results from the model studies;[8] knowledge of the putative crucial transition-state structure (Figure 2) simplifies the problem in two respects: 1) Instead of calculating all relevant stationary points, only the decisive TS and the entrance and exit channels need be calculated. 2) Prior knwoledge of its approximate geometry simplifies locating the TS on an extremely complicated PES. We therefore chose the following strategy to obtain these saddle points while minimizing computational effort: We assumed that the mechanism of Fe^+-mediated C–H bond activation in benzocycloalkenes does not differ in principle from that derived for the small alkane systems ethane and propane, although variations of the geometric features are likely. Hence, we restricted ourselves to calculating concerted transition state structures similar to that known from the model study.[8] Starting from the approximate geometry,[8] we completely reoptimized the saddle points for all reaction channels shown in Figure 1. This procedure ensured that the individual environment of the transition-state structure was taken into account (i.e., additional coordination provided by the benzenoid moiety or steric interaction with other CH_2 units of the ligand, etc).[21] In the following, we will first discuss energetic and then structural aspects of the three potential energy surfaces (PES) investigated.

The Fe^+/tetralin system: Starting from benzocyclohexene (**1**), two primary dehydrogenation products are possible, namely, 1,2-dihydronaphthalene–Fe^+ (**2**–Fe^+), resulting from insertion into the C1–H1 bond followed by formation of TS_{1-2}, and 1,4-dihydronaphthalene–Fe^+ (**3**–Fe^+), produced by insertion into the C2–H2 bond followed by formation of TS_{1-3}. However, only **2**–Fe^+ is found experimentally (Table 1). The structures and relative energies resulting from the DFT calculations are shown in Figure 4.

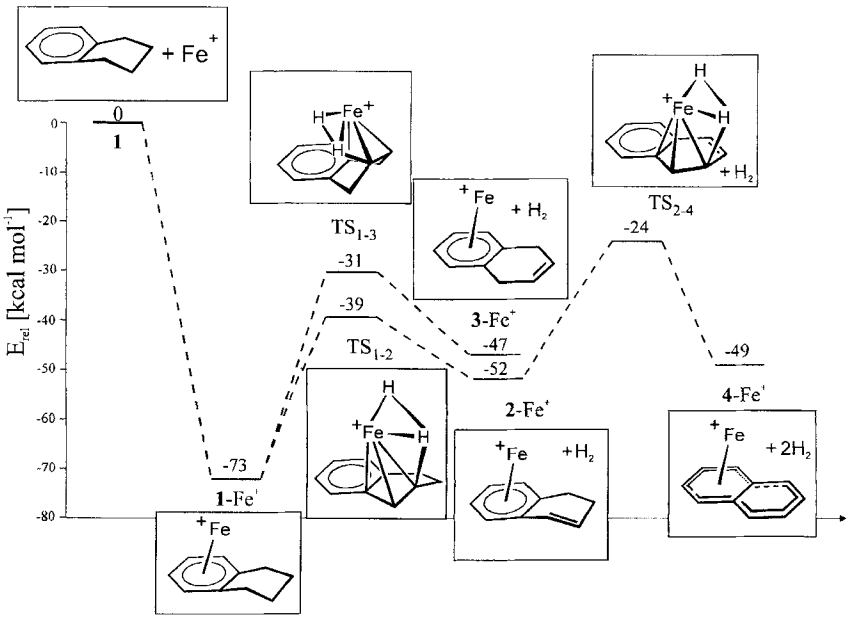

Figure 4. PES for the Fe^+-mediated single and double dehydrogenation of benzocyclohexene.

0947-6539/97/0308-1318 $ 17.50+.50/0 Chem. Eur. J. 1997, 3, No. 8

A common feature of all benzocycloalkene–Fe^+ complexes is, as expected, the η^6 mode of coordination of the iron cation to the benzene subunit, which results in a comparably high bonding energy for the initial complex of 73 kcal mol^{-1}. This energy, which in the isolated system is stored as rovibrational excitation of the encounter complex, is by and large the driving force of the endothermic dehydrogenation. While transition-state structures TS_{1-2} and TS_{1-3} clearly lie below the entrance channel $\mathbf{1}+Fe^+$ (31 and 39 kcal mol^{-1}), the calculations predict TS_{1-2} to be 8 kcal mol^{-1} more stable; this is in qualitative agreement with the experimental observation that dehydrogenation at the C1/C2 position prevails. We also find a TS for the second dehydrogenation, again located below the entrance channel (TS_{2-4}, 24 kcal mol^{-1}), supporting the experimental finding that both single and double dehydrogenations are possible. Looking at the relative stabilities of the minima, we find that the encounter complex $\mathbf{1}$–Fe^+ is the global minimum (73 kcal mol^{-1}). Relative to $\mathbf{1}$–Fe^+, the first dehydrogenation reaction is endothermic by 21 kcal mol^{-1}. Interestingly the second dehydrogenation reaction is endothermic by only a further 3 kcal mol^{-1}; obviously, this reflects the aromatic stabilization of the naphthalene ligand in complex $\mathbf{4}$–Fe^+.

A detailed analysis of the structural features of the minima of tetralin–Fe^+ and its dehydrogenated derivatives was given in our previous study;[9] we therefore give only a short description here. In $\mathbf{1}$–Fe^+ the iron is centered above the aromatic ring, as is also found for benzene–Fe^+.[9, 20] Compared to those in the free ligand, the C–C bonds in the benzenoid substructure are slightly elongated and the C–H bonds are bent out of the plane of the ring by 2°. Also, a Mulliken charge analysis reveals a charge transfer from the ligand to the iron cation of 0.2–0.3 electrons, pointing to a considerable covalent component in the bonding interactions between metal and ligand. Although it must be assumed that the aliphatic ring is polarized by the electric field of the iron cation, this does not seem to affect its equilibrium geometry, since the conformation of the ring as well as bond lengths and angles resemble those of the ligand in the absence of the metal cation. It seems that the six-membered ring (which is in principle analogous to a cyclohexene unit) is not flexible enough to respond to the polarizing effect exerted by the Fe^+ cation.

The features described above for $\mathbf{1}$–Fe^+ are retained in the complexes $\mathbf{2}$–Fe^+, $\mathbf{3}$–Fe^+, and $\mathbf{4}$–Fe^+; this observation further demonstrates the relative rigidity of tetralin (**1**) and its dehydrogenated derivatives. In particular, in none of the dehydrogenated complexes ($\mathbf{2}$–Fe^+, $\mathbf{3}$–Fe^+, and $\mathbf{4}$–Fe^+) can the newly formed double bond(s) get near enough (through conformational changes) to the iron cation for additional complexation. Selected geometrical parameters of the optimized structures of the initial complexes of Fe^+ with **1**, **5**, and **10** are given in Figure 5; the dehydrogenated complexes are shown in Figure 6.

The structures of TS_{1-2} and TS_{1-3} differ fundamentally from the minima ($\mathbf{1}$–Fe^+, $\mathbf{2}$–Fe^+, $\mathbf{3}$–Fe^+, and $\mathbf{4}$–Fe^+) and reveal the reason for the energetic difference between the two saddle points. A summary of the geometrical features of all optimized saddle points is given in Table 2. In both transition states the iron leaves its centered position and moves towards the non-aromatic ring, maintaining some interaction with the benzene ring through η^1 coordination to one of the bridging carbon atoms.

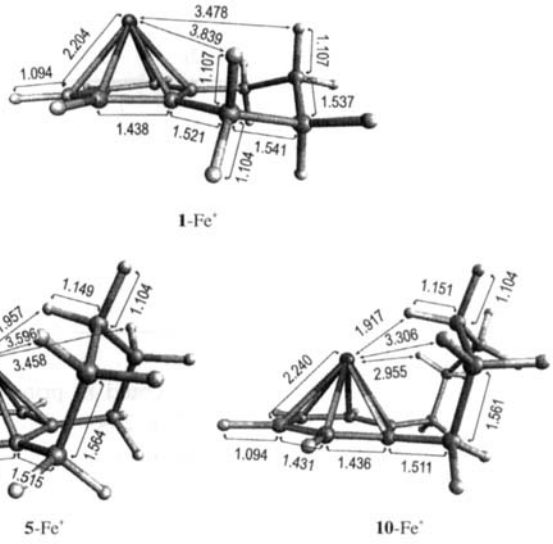

Figure 5. Selected geometrical parameters for initial complexes $\mathbf{1}$–Fe^+, $\mathbf{5}$–Fe^+, and $\mathbf{10}$–Fe^+.

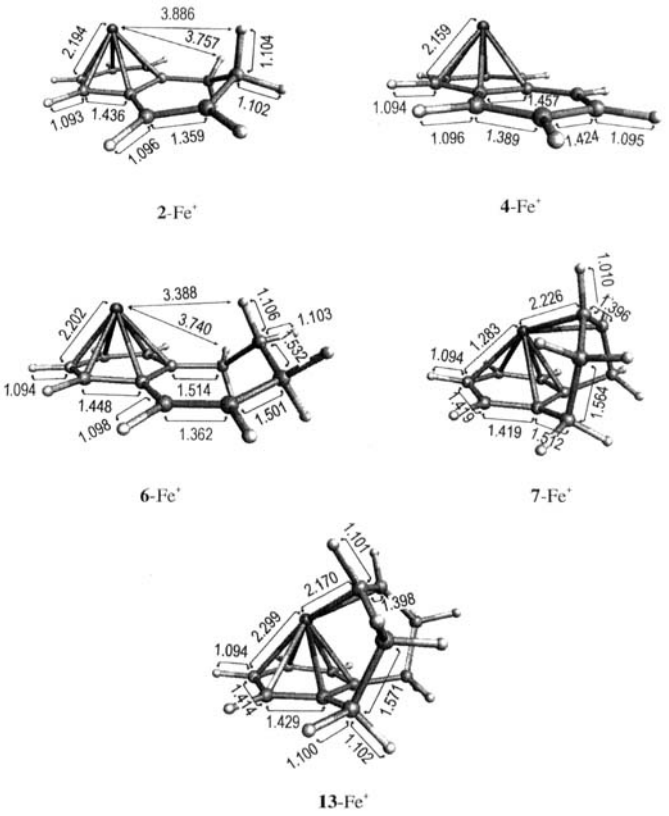

Figure 6. Selected geometrical parameters for the mono- and didehydrogenated Fe^+ complexes.

Unlike $\mathbf{2}$–Fe^+, $\mathbf{3}$–Fe^+, and $\mathbf{4}$–Fe^+, TS_{1-3} contains a non-aromatic ring distorted from the minimum geometry of tetralin. Obviously, two effects are operating here: 1) It is unfavorable for the iron to give up the complexation with the benzene ring entirely by moving to the reaction site; the reaction site must therefore bend towards the iron to some extent. 2) This induces strain in the non-aromatic ring and leads to a higher energy relative to TS_{1-2}, which is formed without significant alteration in the structure of the non-aromatic ring (see Figure 4).

Table 2. Selected geometric features of the calculated transition-state structure. For atom numbering, see Figure 2 (distances in Å, angles in degrees).

	r(Fe-C1)	r(Fe-C2)	r(C1-C2)	r(Fe-H1)	r(Fe-H2)	r(H1-H2)	r(H1-C2)	a(Fe-C1-C2)	a(H1-C2-C1)
TS_{1-2}	2.008	2.228	1.440	1.578	1.578	1.449	1.473	78.7	62.0
TS_{1-3}	2.006	2.173	1.450	1.633	1.589	1.623	1.314	74.3	65.8
TS_{2-4}	2.013	2.289	1.463	1.647	1.574	1.715	1.351	80.7	60.2
TS_{5-6}	2.057	2.198	1.450	1.620	1.590	1.548	1.341	75.4	64.9
TS_{5-7}	2.002	2.243	1.442	1.576	1.577	1.445	1.445	79.5	61.3
TS_{6-8}	2.006	2.295	1.453	1.615	1.579	1.603	1.410	81.4	59.8
TS_{7-9}	2.002	2.208	1.440	1.570	1.579	1.402	1.489	77.9	62.4
TS_{10-11}	1.998	2.255	1.445	1.589	1.583	1.440	1.489	80.0	60.8
TS_{10-12}	2.026	2.165	1.444	1.566	1.573	1.553	1.433	75.1	64.7
TS_{10-13}	2.004	2.194	1.463	1.658	1.601	1.611	1.272	75.6	64.2

It should be noted that **2**–Fe^+ could in principle also be generated by insertion into the C2–H2 bond followed by formation of the characteristic transition state (Figure 2) by interaction with the C1–H1 bond. We have checked this option and found it to be less favorable than TS_{1-2}, probably for the same reasons that apply to TS_{1-3}: the iron cation looses more of its binding interaction with the benzenoid substructure when moving to a more distant reaction site; hence, insertion in proximate regions of the molecule is preferred, given that the aliphatic part molecule is rather inflexible.[22] Similar considerations apply to the benzocycloheptene and -octene systems, discussed below.

In the second hydrogenation step, the geometrical features of TS_{2-4} are similar to TS_{1-2} with regard to coordination of the iron cation. These features are also retained in the structures of TS_{5-6} and TS_{10-11} discussed below. This shows that reaction at the benzylic position as a mechanistic option is largely independent from the aliphatic residue of the molecule. As we will see, however, other mechanistic pathways may be more favorable for kinetic reasons.

The Fe^+/benzocycloheptene system: The initial complex **5**–Fe^+ lies 79 kcal mol^{-1} below the entrance channel. Proceeding from **5**–Fe^+, again, two reaction channels are possible for the dehydrogenation of the saturated ring of **5**. In contrast to what was found for the Fe^+/benzocyclohexene system, the calculated barrier heights for the transition states TS_{5-7} and TS_{5-6} of the two competing primary dehydrogenation reactions are separated by only 1 kcal mol^{-1} (Figure 7). This result compares remarkably well with the experimental data for the product distribution of the two primary products 1,2-benzocycloheptene (**6**) and 2,3-benzocycloheptene (**7**) (42:58). The agreement between theory and experiment in this particular point strengthens our confidence that the assumptions made earlier concerning the crucial steps of the dehydrogenation reaction are valid and indeed transferable to more complicated systems. Also, this example shows that the theoretical approach chosen is capable of predicting the relative barriers of different reaction channels fairly precisely.

For the second dehydrogenation step of the Fe^+/benzocycloheptene system, we focused on two of the three possible paths (cf. Figure 3). The endothermicity for the first dehydrogenation step is in the same range as that found for the Fe^+/benzocyclohexene system—21 kcal mol^{-1} for **6**–Fe^+ and 17 kcal mol^{-1} for **7**–Fe^+. Therefore, **7**–Fe^+ is 4 kcal mol^{-1} lower in energy than **6**–Fe^+ because of additional stabilization with the newly formed double bond. Proceeding from **6**–Fe^+ and **7**–Fe^+, only the reactions involving the benzylic positions need be considered. The dehydrogenation of **6**–Fe^+ at the homobenzylic position is likely to be significantly higher in energy: since the distance between Fe^+ and this reaction site is much larger (see Figure 6) and because of the increased rigidity of **6** due to the double bond formed in the first H_2 elimination, the non-aromatic ring cannot easily change its conformation so as to facilitate insertion into a homobenzylic C–H bond.

The results shown in the right half of the PES in Figure 7 are comparable to those for the Fe^+/tetralin system in that the barriers to the second dehydrogenation (TS_{7-9},

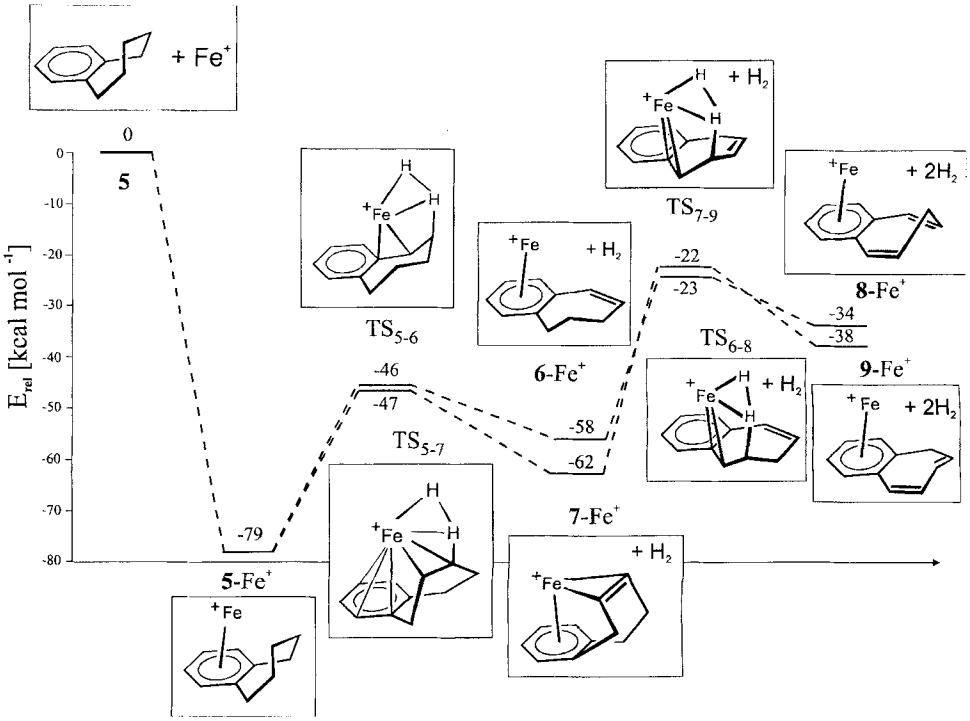

Figure 7. PES for the Fe^+-mediated single and double dehydrogenation of benzocycloheptene.

0947-6539/97/0308-1320 $ 17.50+.50/0 Chem. Eur. J. 1997, 3, No. 8

-22 kcal mol^{-1} and TS_{6-8}, -23 kcal mol^{-1}) are similar to the -24 kcal mol^{-1} found for TS_{2-4} (with respect to the entrance channel). Nevertheless, the second H_2 abstraction is now endothermic by 24 kcal mol^{-1} for the benzocycloheptene system relative to the first dehydrogenation in both cases; this contrasts sharply with the value of only 3 kcal mol^{-1} required in the case of naphthalene–Fe^+ formation (**4**–Fe^+). Can these figures be correlated with the fact that neither **8**–Fe^+ nor **9**–Fe^+ are formed in the gas-phase experiment? The calculated results on the barrier heights imply that, from an energetic viewpoint, consecutive dehydrogenation should be possible for benzocycloheptene, and at first glance there seems to be a discrepancy between experimental and theoretical results. One explanation may be that the non-aromatic ring of the Fe^+/benzocycloheptene system is floppier than the Fe^+/tetralin system and can thus more easily disperse energy by exciting the low vibrational modes. As a consequence, the energy required to overcome TS_{6-8} or TS_{7-9} is no longer available, and further dehydrogenation is thus inhibited. Also, the barrier for a second dehydrogenation with regard to the minima **6**–Fe^+ and **7**–Fe^+ is higher for this system (35 and 40 kcal mol^{-1}, respectively) than for the benzocyclohexene–Fe^+ system (28 kcal mol^{-1}). However, the most probable origin of this apparent contradiction can be traced back to the notorious overbinding tendency of pure DFT methods,[4] which we have estimated to amount to ca. 10 kcal mol^{-1} for equilibrium structures in our previous study.[9] While this applies also to TS_{2-4}, where we found consistency between experiment and theory, it must be suspected that the relative energies for TS_{6-8} or TS_{7-9} lie near or only slightly above the entrance channel, and subtle differences determine whether second dehydrogenation takes place or not. Additional investigations on this subject are currently taking place in our laboratory.[23] Preliminary results employing more sophisticated HF/DFT hybrid approaches assign the energies for TS_{7-9} and TS_{6-8} close to the entrance channel, and in these calculations TS_{2-4} again turns out to be somewhat lower than TS_{7-9} and TS_{6-8}. From these preliminary findings, we draw two major conclusions: The overbinding tendency of pure DFT is most pronounced for transition states and can be reduced by use of DFT/HF hybrid methods. However, what is more important for the scope of the present work, the order of relative energies, for example, for transition states leading to different reaction channels, both methods are in good agreement with the available experimental data.

Inspection of the minimum geometries on this PES reveals similar features to those already found for the benzocyclohexene–Fe^+ system. The iron coordinates with the benzenoid π system leaving the ligand structure nearly unaffected. An exception is **7**–Fe^+ where the iron is actually η^8-coordinated; here, the non-aromatic ring adopts a conformation in which the newly formed double bond can interact with the iron and thus adds additional stabilization to the complex. At this point, we would like to direct the reader's attention to the equilibrium geometry of **5**–Fe^+ (Figure 5). The equatorial hydrogen located at C3 is already rather close to the iron (1.957 Å). Also, since this equatorial C–H bond is stretched relative to the axial one by 0.045 Å, it is apparent that some interaction between the hydrogen atom and the iron cation already exists in the initial complex. This is also corroborated by analysis of the Kohn–Sham molecular orbitals for this complex. Therefore, one could argue that this particular C–H bond is the most likely site for primary insertion of the iron. However, the transition-state structure that follows insertion into the C–H bond located at C2 (i.e. TS_{5-7}) is energetically more favorable for steric reasons than the one resulting from insertion into C3. Moreover, we find that the conformation in which the H atom located at C2 points towards the iron, instead of the H atom at C3, is almost isoenergetic; this suggests that before forming TS_{5-7}, **5**–Fe^+ changes its conformation to facilitate insertion into the C–H bond at C2, resulting in an energetically lower TS. This in turn implies that the lowest-energy conformation of the non-aromatic ring in the initial complex is not necessarily the one adopted in the TS. It also demonstrates that, once the non-aromatic part of the ligand becomes more flexible, geometric arguments derived from the initial minima alone can be misleading when used to predict reactions.

Examination of the geometries of TS_{5-7} and TS_{5-6} reveals the following: TS_{5-6} is very similar to TS_{1-2} as far as the Fe^+ coordination is concerned (see above). The iron is positioned perpendicular to the surface of the benzene ring above one of the bridging carbon atoms, allowing some interaction with the benzene ring in the transition-state structure; at the same time no strain is built up in the non-aromatic ring through energetically demanding conformational changes. In contrast, in TS_{5-7} the iron has only slightly migrated from the central position above the benzene ring. The non-aromatic ring is large and flexible enough to offer the C2/C3 C–H bonds as reaction sites without the iron having to disengage from the benzenoid π system. Owing to the increased flexibility of the non-aromatic ring in **5**–Fe^+, it is clear why the transformation to TS_{5-7} involves a lower barrier. In contrast, for the homologue TS_{1-3}, the iron cation has to sacrifice most of its stabilizing interaction with the benzene ring because of the rigidity of the six-membered non-aromatic ring. As a result, the energetic gap calculated for TS_{1-3} and TS_{1-2} is reduced for the analogous transition-state structures TS_{5-6} and TS_{5-7} so that they are almost isoenergetic.

The Fe^+/benzocyclooctene system: Increasing the alicyclic ring size by one more CH_2 unit results in a larger number of possible dehydrogenation products (three instead of two). Yet, as mentioned above (Table 1 and Figure 1), only one of the three possible primary products is formed. At first sight it is surprising that only C–H bonds at C3/C4 are involved in dehydrogenation. The relative energies of the three transition states (Figure 8) support the experimental findings.

For benzocyclooctene (**10**) the largest interaction energy between the iron cation and the ligand is predicted (82 kcal mol^{-1}); this is due to the increased polarization in the ligand, but also to intramolecular solvation effects, since the ligand structure suggests that a cavity is formed in which the metal ion is embedded and interacts with several ligation points. Of the three transition-state structures located, TS_{10-13}, connecting **10**–Fe^+ with the experimentally observed dehydrogenated product **13**–Fe^+, is the lowest in energy. The other two transition states are higher in energy by 6 (TS_{10-11}) and 21 kcal mol^{-1} (TS_{10-12}). The reaction from **10**–Fe^+ to **13**–Fe^+ H_2 is endothermic by 8 kcal mol^{-1}, which is significantly

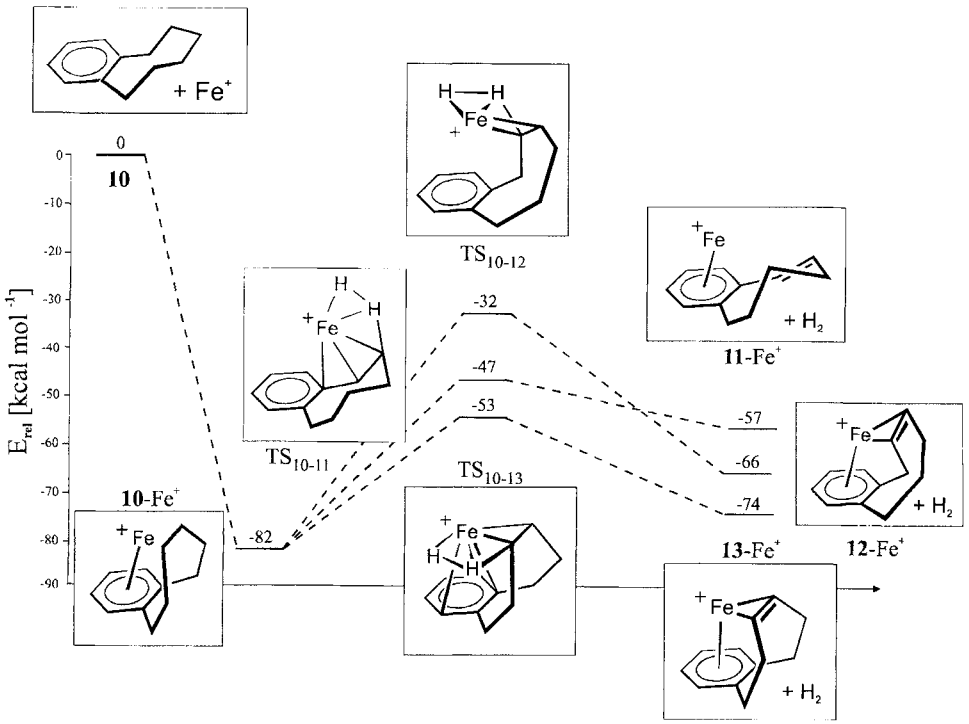

Figure 8. PES for the Fe^+-mediated single dehydrogenation of benzocyclooctene.

lower than found for the first dehydrogenation steps of **1**–Fe^+ and **5**–Fe^+ (17–21 kcal mol^{-1}).

The structural features of the Fe^+ complexes of benzocyclooctene (**10**) differ from those discussed above. The aliphatic part of the molecule is much more flexible and has a multitude of almost isoenergetic conformations. Thus, the shape of the aliphatic part of the molecule now responds markedly to the polarizing effect upon complexation with Fe^+ in all but one case (TS_{10-12}, cf. Figure 8), in order to maximize interaction between the Fe^+ and the organic ligand. The conformation of the non-aromatic eight-membered ring of benzocyclooctene (**10**) changes from being more or less flat to a folded three-dimensional shape, almost surrounding the iron cation. Inspection of the geometries of TS_{10-11}, TS_{10-12}, and TS_{10-13} reveals that, owing to a transannular effect with the C3/C4 position of the non-aromatic ring, in TS_{10-13} the iron cation remains practically unperturbed in its η^6 bonded interaction above the benzene ring. At the same time, formation of this transition state proceeds without inducing significant strain in the non-aromatic ring, as the conformation of the alicyclic part also remains largely unperturbed. In fact, the shape of the whole molecule hardly changes from **10**–Fe^+ to TS_{10-13}. This corresponds to the energetically ideal case discussed earlier. The opposite is true for TS_{10-12} (reaction at the C2–C3 positions). The fact that this transition-state structure is by far the highest in energy can be rationalized by means of its geometrical features[24]—it represents the worst case discussed above: Because of the large distance between the iron cation and the reaction site, the iron has to leave its position above the benzene ring completely and migrate to the reaction site. This is due to the fact that the non-aromatic ring cannot adopt a conformation that is relatively low in energy and at the same time allows the iron to retain its interaction with the aromatic π system.[25] For TS_{10-11} (reaction in the benzylic position) the situation resembles those of TS_{1-2} and TS_{5-6}. With regard to the possible dehydrogenated products, **11**–Fe^+ (double bond in the benzylic position) shows the same features as its lower homologues. The energetically lowest structure (**13**–Fe^+) and also **12**–Fe^+ can achieve additional stabilization by coordination of the transannular double bond with the iron cation. In the transformation of **10**–Fe^+ via TS_{10-13} to **13**–Fe^+, the conformation of the atoms not taking part in reaction changes very little; this explains the low barrier and moderate endothermicity of the dehydrogenation reaction, but also the high preference for this reaction channel.

Since none of the possible secondary dehydrogenation products for **10**–Fe^+ were observed experimentally and in view of the size and complexity of this system, the corresponding structures were not calculated.

Conclusions

In a combined experimental and theoretical approach the differences in the chemical behavior of the Fe^+-mediated dehydrogenation of benzocyclohexene, benzocycloheptene, and benzocyclooctene have been explored. Extensive mass spectrometric labeling experiments show that increasing the size of the alicyclic ring results in a shift from reactions at the benzylic position to remote activation of the transannular C–H bonds. Density functional calculations fully support the experimental results, assigning the lowest activation barriers to the reaction channels that lead to the experimentally observed reaction products in every case. The relative stabilities are well reproduced by the DFT approach chosen, thus affording a consistent picture with the available experimental data. However, the energetic information with regard to the entrance channel is less accurate, due to the overbinding tendency inherent in pure DFT functionals. More accurate calculations, employing HF/DFT hybrid functionals, and application of refined population analysis schemes, such as natural bond orbital analysis, to gain more insight into the bonding situation are desirable and will be published in due course.[23]

The structural and energetic information together with the experimental observations unequivocally suggest a general underlying pattern for the regioselectivity of C–H bond activation in these systems. When the size of the non-aromatic ring is increased from six to eight carbon atoms, the molecule changes from a rather rigid (benzocyclohexene) via a modestly flexible (benzocycloheptene) to a rather floppy system (benzocyclooctene). The iron cation, which is bound to the benzene moiety of the molecule, prefers reaction sites that allow it to maintain its interaction with the benzene anchor to the greatest

0947-6539/97/0308-1322 $ 17.50+.50/0 Chem. Eur. J. 1997, 3, No. 8

extent possible. If the non-aromatic ring is flexible enough to bring remote reaction centers into the vicinity of the metal center by conformational changes without inducing too high a strain energy, remote activation will occur, as seen for benzocyclooctene (**10**). If the non-aromatic ring is small and rigid, as in benzocyclohexene **1**, reaction will occur in the benzylic C1/C2 position, allowing the iron to maintain at least part of its interaction with the benzene ring. Between these extremes, both mechanisms compete, as is seen for benzcycloheptene. Here, remote bond activation takes place with a slight migration of Fe^+ from its central position above the benzene ring; this enables formation of the characteristic transition state without necessitating disengagement of Fe^+ from its anchored position. The competing mechanisms cause the barriers of different reaction channels to be almost energetically degenerate, and the product ratio shifts from the exclusive formation of only one isomer to a mixture of isomers.

Acknowledgments: R. H. H. thanks Dr. G. Fitzgerald for providing a generous grant of CPU time on the CRAY Research computing facilities and for helpful comments. We are grateful to the Konrad-Zuse-Zentrum für Informationstechnik, Berlin, for additional significant computing resources and excellent service by Dr. T. Steinke. Dr. M. Holthausen and Dipl.-Chem. T. K. Dargel are acknowledged for helpful discussions. This work has benefited from funding by the Deutsche Forschungsgemeinschaft, the Volkswagen Stiftung, the Fonds der Chemischen Industrie, and the Gesellschaft von Freunden der Technischen Universität Berlin.

Received: December 5, 1996 [F 538]
Revised version: April 4, 1997

[1] J. Allison, R. B. Freas, D. P. Ridge, *J. Am. Chem. Soc.* **1979**, *101*, 1332
[2] See, e.g.: a) K. Eller, H. Schwarz, *Chem. Rev.* **1991**, *91*, 1121. b) P. B. Armentrout in *Selective Hydrocarbon Activation* (Eds.: J. A. Davies, P. L. Watson, J. F. Liebman, A. Greenberg), VCH, New York, **1990**. c) J. C. Weisshaar, *Acc. Chem. Res.* **1993**, *26*, 213. d) J. A. Martinho Simões, J. L. Beauchamp, *Chem. Rev.* **1990**, *90*, 629. e) D. Schröder, H. Schwarz, *Angew. Chem. Int. Ed. Engl.* **1995**, *34*, 1973
[3] See, e.g.: a) *The Challenge of d and f Electrons, Theory and Computation* (Eds.: D. R. Salahub, M. C. Zerner), ACS Symposium Series 394, American Chemical Society, Washington DC, **1989**. b) C. W. Bauschlicher, Jr., S. R. Langhoff, H. Partridge in *Modern Electronic Structure Theory, Part II*, World Scientific, Singapore, **1995**.
[4] For monographs and reviews on density functional theory, see, e.g.: a) *Density Functional Methods in Chemistry* (Eds.: J. K. Labanowski, J. W. Andzelm), Springer: New York, **1991**. b) T. Ziegler *Chem. Rev.* **1991**, *91*, 651. c) *Modern Density Functional Theory: A Tool for Chemistry* (Eds.: J. M. Seminario, P. Politzer), Elsevier, Amsterdam, **1995**.
[5] a) J. Hrušák, R. H. Hertwig, D. Schröder, P. Schwerdtfeger, W. Koch, H. Schwarz, *Organometallics*, **1995**, *14*, 1284. b) R. H. Hertwig, W. Koch, D. Schröder, H. Schwarz, J. Hrušák, P. Schwerdtfeger, *J. Phys. Chem.* **1996**, *100*, 12253. c) R. H. Hertwig, J. Hrušák, D. Schröder, W. Koch, H. Schwarz, *Chem. Phys. Lett.* **1995**, *236*, 194. d) C. Heinemann, R. H. Hertwig, R. Wesendrup, W. Koch, H. Schwarz, *J. Am. Chem. Soc.* **1995**, *117*, 495.
[6] a) M. C. Holthausen, C. Heinemann, H. H. Cornehl, W. Koch; H. Schwarz, *J. Chem. Phys.* **1995**, *102*, 4931. b) M. C. Holthausen, M. Mohr, W. Koch, *Chem. Phys. Lett.* **1995**, *240*, 245. c) A. Ricca, C. W. Bauschlicher, Jr., *ibid.* **1995**, *245*, 150. d) A. Ricca, C. W. Bauschlicher, Jr., *Theor. Chim. Acta* **1995**, *92*, 123; f) A. Ricca, C. W. Bauschlicher Jr., *J. Phys. Chem.* **1995**, *99*, 5922; e) V. Barone, *Chem. Phys. Lett.* **1995**, *233*, 129; f) V. Barone, *J. Phys. Chem.* **1995**, *99*, 11659; g) C. Adamo, F. Lelj, *Chem. Phys. Lett.* **1995**, *246*, 463; h) V. Barone, C. Adamo, *J. Phys. Chem.* **1996**, *100*, 2094.
[7] W. Koch, R. H. Hertwig in *The Encyclopedia of Computational Chemistry*, Wiley, New York, in press.
[8] a) M. C. Holthausen, A. Fiedler, H. Schwarz, W. Koch, *Angew. Chem. Int. Ed. Engl.* **1995**, *34*, 2282; *J. Phys. Chem.* **1996**, *100*, 6236. b) M. C. Holthausen, W. Koch, *Helv. Chim. Acta*, **1996**, *79*, 1939.
[9] K. Seemeyer, R. H. Hertwig, J. Hrušák, W. Koch, H. Schwarz *Organometallics*, **1995**, *14*, 4409.
[10] a) R. Srinivas, D. Sülzle, W. Koch, C. H. DePuy, H. Schwarz *J. Am. Chem. Soc.* **1991**, *113*, 5970. b) R. Srinivas, D. Sülzle, T. Weiske, H. Schwarz, *Int. J. Mass Spectrom. Ion Processes* **1991**, *107*, 369. c) K. Seemeyer, Ph.D. Thesis. Technische Universität Berlin, D 83, 1996.
[11] a) J. C. Slater, *Phys. Rev.* **1951**, *81*, 285. b) S. J. Vosko S. J. L. Wilk, M. Nusair, *Can. J. Phys.* **1980**, *58*, 1200. For a more recent and simpler formulation, see also: J. P. Perdew, Y. Wang, *Phys. Rev. B* **1992**, *45*, 13244. c) O. Gunnarson, I. Lundqvist, *Phys. Rev. B* **1977**, 4274.
[12] A. D. Becke, *Int. J. Quantum Chem.* **1983**, *23*, 1915; *J. Chem. Phys.* **1986**, *84*, 4524; *Phys. Rev. A*, **1988**, *38*, 3098.
[13] J. P. Perdew, *Phys. Rev. B* **1986**, *33*, 8822.
[14] MNDO94, Version 4.1, W. Thiel, Organisch-Chemisches Institut, Universität Zürich, CH-8057 Zürich, Switzerland, 1994.
[15] UniChem/DGAUSS Version 3.0, Cray Research, Inc; Eagan, USA **1995**.
[16] N. Godbout, D. R. Salahub, J. Andzelm and E. Wimmer, *Can. J. Chem.* **1992**, *70*, 560.
[17] K. Seemeyer, T. Prüsse, H. Schwarz, *Helv. Chim. Acta* **1993**, *76*, 113.
[18] D. R. Salahub in *Ab Initio Methods in Quantum Chemistry, Part II* (Ed.: Lawley), Advances in Chemical Physics, Vol. LXIX, Wiley, Chichester, **1987**, p. 447.
[19] J. Baker, A. Scheiner, J. Andzelm, *Chem. Phys. Lett.* **1993**, *216*, 380.
[20] C. W. Bauschlicher, Jr., H. Partridge, S. R. Langhoff, *J. Am. Chem. Soc.* **1992**, *96*, 3273.
[21] An approximate optimization procedure, in which the coordinates of the five-membered transition-state structural element were kept frozen while the rest of the molecule was optimized, was not found to be successful, since only the coordinates of the transition-state structural element (i.e. those shown in Figure 3, Table 2) are known from the model study. Other geometrical parameters which would also have to be kept frozen in such a restricted optimization, such as the distance between the iron cation and the benzenoid moiety of the molecule, are not known a priori. However, this distance is decisive in determining the relative energy of the structure. Therefore, we deemed it necessary to completely optimize the geometries of all transition-state structures.
[22] One of the reviewers pointed out that through ring slippage reactions the benzenoid part could loose its planarity upon change of hapticity of the metal–benzene bond, as found by J. M. O'Conner, C. P. Casey, *Chem. Rev.* **1987**, *87*, 307 and T. G. Traylor, K. J. Stewart, *J. Am. Chem. Soc.* **1986**, *108*, 6977. Such a distortion of the aromatic unit was, however, not found in the present calculations even though the benzene ring was not forced to maintain its planarity.
[23] R. H. Hertwig, W. Koch, unpublished results.
[24] We were not able to fulfill the geometry convergence threshold entirely for the structure of TS_{10-12}, probably owing to weak interactions between the iron cation and the benzenoid substructure.
[25] Different conformations for $TS_{10\ 12}$ have been checked; however, a saddle point could not be located in any other case.